Journal of Structural Geology, Vol. 14, No. 1, pp. 19 to 28, 1992
Printed in Great Britain

0191-8141/92 $05.00+0.00

Domainal failure of serpentinite in shear zones, State-Line mafic complex, Pennsylvania, U.S.A.

ALEXANDER E. GATES

Department of Geology, Rutgers University, Newark, NJ 07102, U.S.A.

(*Received* 4 *February* 1991; *accepted in revised form* 26 *May* 1991)

Abstract—Deformation within 0.2–1.4 km wide dextral strike-slip shear zones in the serpentinite portion of the State-Line mafic complex, Pennsylvania–Maryland, is partitioned into two types. Anastomosing throughgoing mylonitic faults experienced a long, relatively simple deformational history of unidirectional dextral transcurrent shearing. The relatively less deformed, lenticular shaped areas between these faults deformed in a complex sequence of faulting. The lenticular pods contain early E-striking extensional veins and brittle reverse faults with north strikes. Northeast-striking dextral strike-slip faults deformed the veins and reverse faults. East-striking shear bands developed in both the throughgoing faults and the mylonitic dextral faults within the lenticular pods. Northwest-striking sinistral strike-slip faults transected the lenticular pods and earlier faults. The sinistral mylonites formed shear bands late in their movement history. A similar sequence of faulting occurred in microscopic lenticular pods within mylonitic serpentinite. These faults exhibit the same orientation and sequence as their larger counterparts but are clearly not synchronous with them. Each lenticular pod may have acted as a separate system, and therefore like faults between pods of any size may not have been synchronous.

INTRODUCTION

SERPENTINITE bodies characteristically display complex deformation histories and geometries. Williams (1979) recognized a composite texture of serpentinite in the Peel Fault, New South Wales. Phacoids of massive serpentinite are enclosed within anastomosing bands of schistose serpentinite. Multiple fault sets with sequential activity were found in the serpentinite. In another part of the Peel Fault, Katz (1986) proposed Riedel shearing to explain the complex brittle fault patterns in the Woodsreef serpentinite. This interpretation is based on the orientations and observed or inferred relative movement senses of slickensides. O'Hanley (1987) proposed that multiple orientations and overprinting relations of cross-fiber veins in the Thetford asbestos mines in southeastern Quebec reflect rapidly changing stress orientations. Faults and veins in the Cassiar Mine, British Columbia, as well as those in the Woodsreef and Thetford Mines, record a change from reverse to strike-slip movement early in the deformation history (O'Hanley 1988).

The serpentinite portion of the State-Line mafic complex contains several 0.2–1.4 km wide shear zones (Gates & Kambin 1990, Gates in press). Each shear zone is composed of a series of thin anastomosing mylonitic faults that enclose lenticular areas or pods of undeformed to variably deformed serpentinite. Whereas the anastomosing faults underwent unidirectional ductile flow during deformation, the lenticular pods deformed through a complex interaction of sequential faulting. In this study, the enclosing faults and lenticular pods are described, evidence for the sequence of faulting in the lenticular pods is presented, and a model for failure of serpentinite in shear zones is proposed.

GEOLOGY OF THE STATE-LINE SERPENTINITE

The State-Line mafic complex underlies part of the Pennsylvania–Maryland Piedmont and is the northernmost portion of the Baltimore mafic complex, U.S.A. (Fig. 1). Lapham & Bassett (1964) proposed that the State-Line complex intruded the Piedmont during the Taconic orogeny, based on K/Ar dating of the inferred contact aureole. The entire Baltimore mafic complex was later proposed to be an ophiolite that was emplaced onto North America during the Taconic orogeny (Crowley 1976, Morgan 1977, Wagner & Srogi 1987). However, Nd/Sm studies of rocks from the Maryland Piedmont indicate that the Baltimore mafic complex intruded through continental crust at approximately 490 Ma (Shaw & Wasserburg 1984). Recent petrologic and geochemical studies suggest that the State-Line complex is a layered mafic intrusion (Hanan & Sinha 1989, Gates in press, Gates *et al.* in press). The serpentinite is the metamorphosed ultramafic base of the intrusion.

The State-Line complex is a 2.2–2.7 km thick plate that dips 24° to the southeast (Gates & Sun 1989). It is mainly composed of gabbro but the roof portion is quartz gabbro and diorite with xenoliths of metasedimentary country rock and granite and aplite dikes. The lower part is dominantly serpentinized peridotite with minor relict dunite, wehrlite and websterite. The State-Line complex overlies quartzite-rich metasedimentary rocks of the Peters Creek Formation in fault contact.

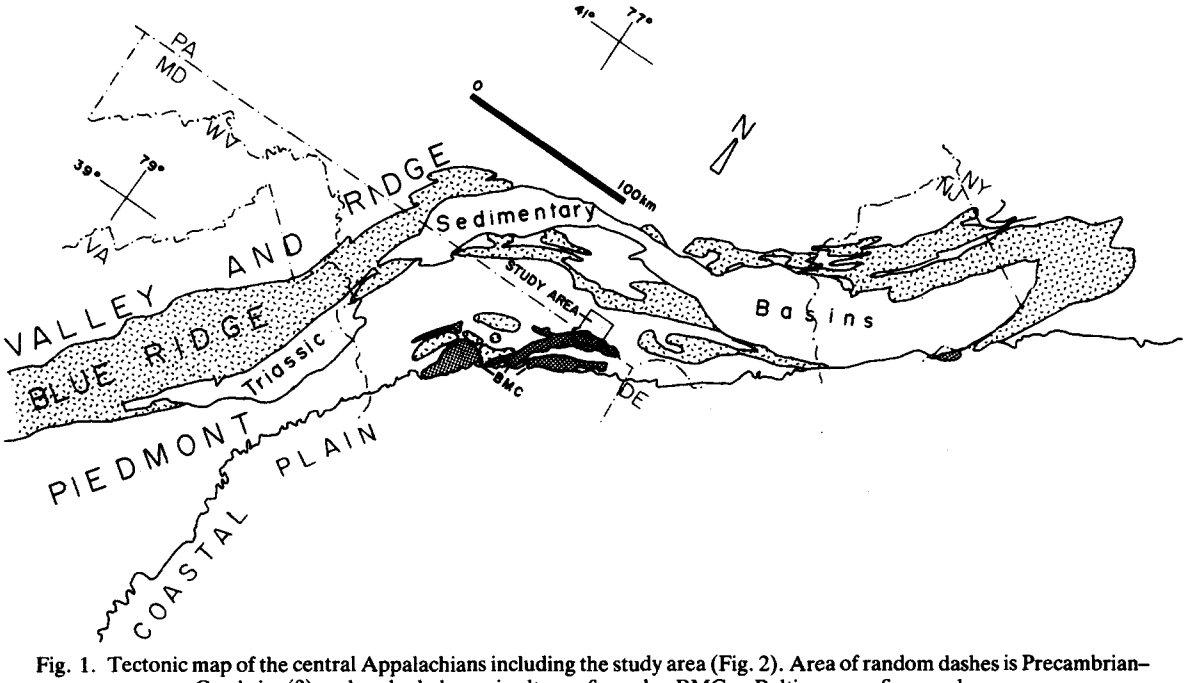

Fig. 1. Tectonic map of the central Appalachians including the study area (Fig. 2). Area of random dashes is Precambrian–Cambrian(?) rocks; shaded area is ultramafic rocks; BMC = Baltimore mafic complex.

The quartzite-rich rocks are gradational into the underlying metapelite-rich portion of the Peters Creek Formation (Gates *et al.* in press).

Shear zones

The serpentinite (ultramafic) portion forms a 0.5–2.0 km wide rim along the northern contact of the State-Line complex (Fig. 2). A series of NE-trending dextral transcurrent shear zones of 0.2–1.4 km width cross the serpentinite. The shear zones consist of anastomosing bands of well foliated, fine-grained mylonitic serpentinite. Lenticular pods of weakly deformed serpentinite form the areas between the anastomosing mylonitic bands. These pods range in size from several millimeters to several hundred meters.

The mylonitic serpentinites are well-foliated *L–S* tectonites (types 2, 4 and 8 of Wicks & Whittaker 1977) with few relict minerals and textures. Petrographically, they exhibit a mesh to ribbon texture (Maltman 1978) in which the cord areas (flow foliation) have undergone grain size reduction and strong alignment of recrystallized serpentine (Fig. 3a). The cord areas are composed of lizardite with minor talc and chrysotile (Gates & Kambin 1990). The core areas are mm-scale weakly deformed lenticular pods.

Kinematic indicators are abundant in the serpentinite mylonites. Serpentine fibers and plates at the edges of the lenticular pods show drag into the surrounding mylonitic foliation (Fig. 3b). The mylonitic foliation commonly exhibits *S*- and *C*-planes (Berthé *et al.* 1979, Norrell *et al.* 1989) on the microscopic scale (Fig. 3c). Early formed foliation is defined by lizardite, talc and chrysotile (*S*-planes), and is cross-cut by and dragged into late *C*-planes which contain the same minerals (Gates & Kambin 1990). In the well developed mylonites, *C*- and *S*-planes are parallel or subparallel and are commonly indistinguishable. Many of the mylonites contain d-type (ductile) and less commonly f-type (fracture) shear bands (see Norrell *et al.* 1989) (Fig. 3d). The shear bands are oriented at 20–25° to the *C*-planes and show movement sense by drag and offset of the mylonitic foliation and veins. The d-type shear bands are defined by finely recrystallized lizardite, chrysotile and talc. The fibrous serpentine lineations on the mylonites also yield movement orientation.

The serpentinite is replaced by assemblages of talc and magnesite in the central parts of some of the wider mylonite zones (Gates & Kambin 1990, Gates in press). In these rocks rotated clasts of lizardite-rich mylonitic serpentinite exhibit retrograde metamorphic reactions to the matrix of sheared talc with minor magnesite. The talc–magnesite matrix forms an *S–C* mylonite and with rotated serpentinite clasts shows an unequivocal movement sense. In cases where magnesite is the dominant or sole matrix component, the mylonitic serpentinite forms brecciated clasts. The magnesite matrix is finely recrystallized in bands that are parallel to the mylonitic foliation.

The lenticular pods are composed of weakly-deformed massive serpentinite which is similar to the serpentinite outside the shear zones. The massive serpentinite exhibits mesh and/or bladed mat textures (Maltman 1978), and unlike the mylonite is dominated by antigorite with lesser amounts of chrysotile, lizardite and talc (Gates & Kambin 1990). It also contains abundant relict minerals including olivine, hypersthene, augite, magnetite and chromite.

Faults within the lenticular pods include thin mylonites, brittle faults with slickensides and combinations of the two. The response of rocks to deformation correlates with mineralogy, pre-existing textures and observable metamorphic reactions (Gates & Kambin 1990). Antigorite-rich serpentinite exhibits brittle faulting

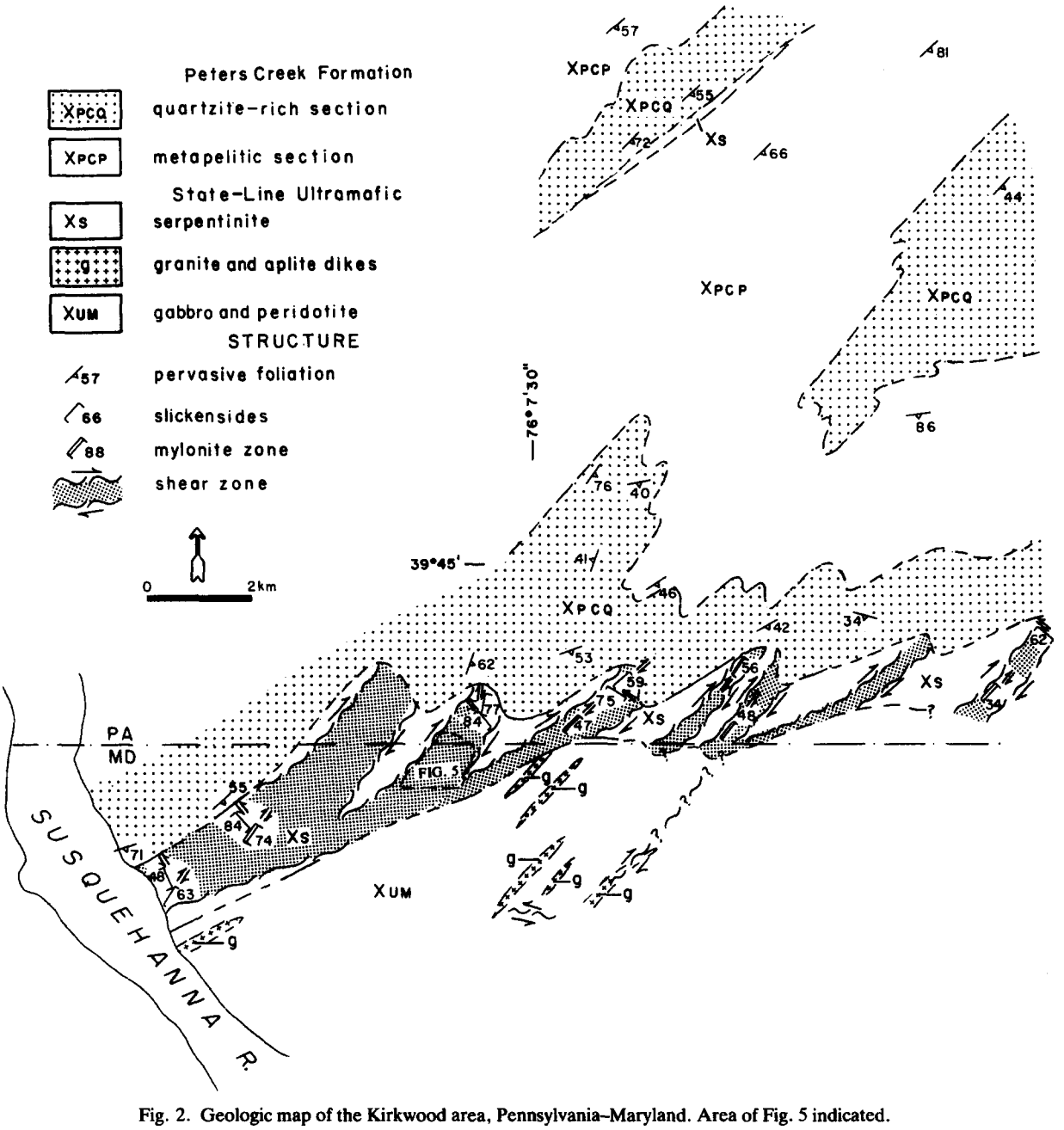

Fig. 2. Geologic map of the Kirkwood area, Pennsylvania–Maryland. Area of Fig. 5 indicated.

whereas lizardite-rich serpentinite primarily exhibits ductile faulting depending upon the texture. Faults in which antigorite reacted to form lizardite were also ductile.

Sense of movement is best determined in the rare faults that offset veins and pre-existing faults. The most common brittle kinematic indicators are slickensides. Fibrous slickensides with terminations yield unequivocal movement senses and movement orientations. The slickensides exhibit a ribbon texture (Maltman 1978) and contain slip-fibers of chrysotile, antigorite, lizardite and minor talc (Gates & Kambin 1990). Non-asbestiform veins of both lizardite and antigorite commonly contain polished slickensides (types 4 and 8 of Wicks & Whittaker 1977) that only locally exhibit terminations.

STRUCTURES WITHIN THE SHEAR ZONES

The deformational history of the shear zones in the State-Line serpentinite is complex. The main anastomosing mylonite zones exhibit a relatively simple history approximating unidirectional dextral transcurrent shearing. The lenticular pods, on the other hand, exhibit a complex history of sequential faulting. The lenticular pods occur on many scales ranging from millimeters in the core areas of the mylonitic serpentinite (Figs. 3a and 4a & b) to mappable bodies of several hundred meters (Fig. 5). Although the succession, orientation and movement sense of the faults is similar in all of the deformed lenticular pods, they are not necessarily synchronous in different pods (discussed later). In this analysis, faults from all areas are therefore grouped

based on type and succession rather than absolute timing.

The succession of faulting in the lenticular pods is determined through overprinting relations including younger faults that offset older faults, drag of older faults into the younger ones, metamorphic reactions, and successive overprinting of slickensides. Overprinting relations were determined primarily on outcrop.

Sinistral strike-slip faults

Sinistral strike-slip faults overprint all other faults in the lenticular pods. Overall, they appear to have undergone the least amount of subsequent reorientation. These faults occur both as mylonites and slickensided fault planes. They range in width from a single plane (1–2 mm) for brittle faults, to 3–4 m for mylonite zones. The wider zones are more common in the larger pods. The mylonite zones generally strike NW and dip moderately to steeply both to the northeast and southwest, but the orientations of the faults are variable (Figs. 5 and 6a). Fault striations and mineral lineations indicate movement towards 300–310° and 120–130° with plunges of 0–30° which indicate strike-slip to oblique strike-slip motion. The average movement is pure sinistral strike-slip on a steeply SW-dipping plane. Rare shear bands occur in a few of the mylonites and are oriented at approximately −20° to the shear zone boundary, or west-northwest. Where best developed, the shear bands are spaced 3–5 cm apart.

Dextral strike-slip faults

The anastomosing mylonite zones that bound the lenticular pods exhibit dextral strike-slip motion. These zones are as much as 8 m thick. Dextral strike-slip faults are also common within the lenticular pods. They range in width from single slickenside planes to 3–4 m for mylonite zones. Discrimination of bounding shear zones from dextral transcurrent zones within pods is difficult on outcrop scale. They have similar compositions, appearances and orientations. Both fault types are therefore included in the general description of dextral transcurrent faults and discriminated in the description of the pods.

Like the sinistral faults, the dextral faults anastomose, resulting in variations in their orientations (Figs. 5 and 6b). In addition, later reorientation of the faults within lenticular pods as the result of drag into sinistral faults further complicates the angular relations. The average orientation of the dextral faults is 035–045°, 60–75°SE but ranges from 010° to 060° with moderate to steep dips both to the southeast and northwest. Slip lineations are similarly variable but generally trend NE–SW and plunge ≤35°. The resultant motion is approximately dextral strike-slip on a steeply SE-dipping fault plane.

The dextral mylonite zones commonly exhibit shear bands. The shear bands are spaced at 1–3 cm and oriented at +20–25° to the *C*-plane mylonitic foliation and to the shear zone boundaries where observable (Figs. 5 and 6c). The shear bands strike ENE to E and dip moderately to steeply towards the southeast. Their orientations vary because they occur in anastomosing zones and were reoriented where overprinted by sinistral faults.

Cross-fiber veins

Cross-fiber serpentine veins were among the earliest structures formed. There are many generations of veins with a variety of orientations within the lenticular pods but the early formed veins are generally wider (up to 2 cm) than the later sets and contain well developed serpentine fibers. Commonly, the veins are highly deformed (Fig. 4b) but are rarely intact in areas with little subsequent shearing. The veins exhibit a variety of orientations as a result of later deformation (Fig. 5). The least deformed veins strike 048–090° and are nearly vertical. There are also several examples of 1–2 cm wide cross-fiber veins with NNE strikes. The relative age of these veins, however, could not be determined.

Reverse faults

Small, dominantly brittle reverse faults are common in the lenticular pods. The reverse faults are deformed by all strike-slip faults where they occur together. The reverse faults have variable orientations but they are dominantly steeply dipping and strike approximately 355–020° in areas with few strike-slip faults. The vast majority of the reverse faults were reoriented or reactivated by the later faulting.

Relative timing of faults

In rare cases the central portions of wide, throughgoing dextral mylonitic faults show retrograde metamorphic reactions. Mylonitic, lizardite-rich serpentinite is replaced by assemblages of sheared talc and magnesite. The talc–magnesite rocks also show a dextral strike-slip shear sense. Gates & Kambin (1990) showed that the talc–magnesite assemblages formed at lower temperatures than the lizardite assemblages. Because the talc–magnesite rocks clearly post-date the serpentinite mylonites and they only occur in dextral strike-slip faults, dextral strike-slip faulting in the wider mylonite zones is interpreted to post-date all other activity in the shear zones of the State-Line serpentinite.

Although brittle dextral and sinistral faults appear to be conjugate in some of the lenticular pods, the dextral mylonite zones including dextral shear bands were reoriented where they intersected sinsitral mylonite zones. The strikes of the dextral mylonite zones progressively swing from the typical northeast direction counterclockwise towards the northwest and parallel to the sinistral faults in proximity to the sinistral faults (Figs. 4b and 7a & b). The swing is caused by drag on the sinistral faults and is more pronounced adjacent to mylonitic faults or concentrated brittle faults. Drag folds are formed with steeply plunging fold axes in the dextral faults (Fig. 7b).

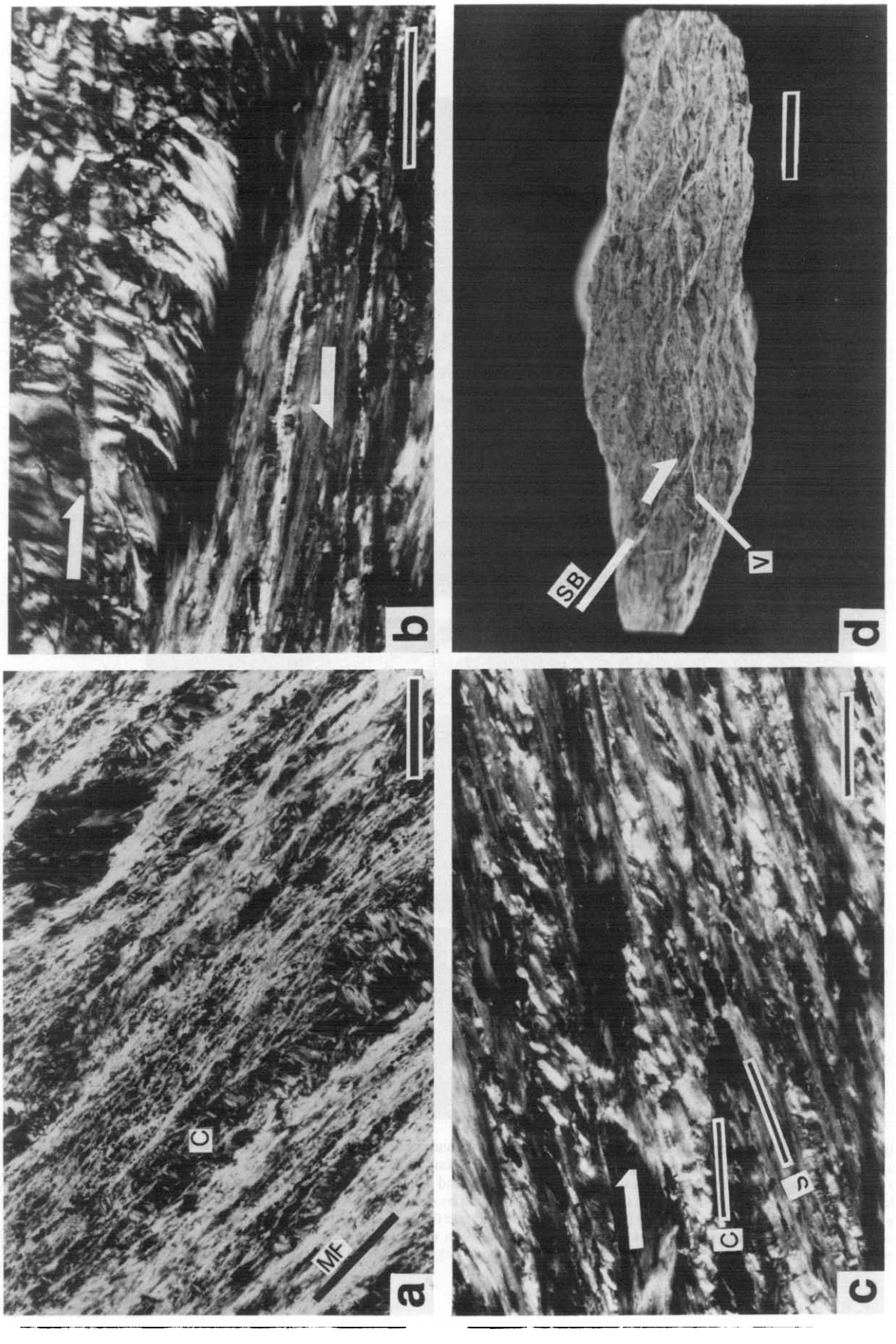

Fig. 3. Textures in mylonitic serpentinites. (a) Photomicrograph of mylonitic serpentinite. **MF** = mylonitic foliation; **C** = core area composed of bladed mat textured serpentinite, scale bar = 1 mm. (b) Photomicrograph of core (lenticular pod) edge showing drag into mylonitic foliation (arrow shows offset). Scale bar = 0.2 mm. (c) Photomicrograph of *S–C* mylonite (as marked) in lizardite-rich serpentinite. Arrow shows offset direction; scale bar = 1 mm. (d) Shear bands (SB) crossing mylonitic foliation in serpentinite. Cross-fiber chrysotile vein (V) is offset across shear bands in a consistent dextral sense as shown by arrow. Scale bar = 1 cm.

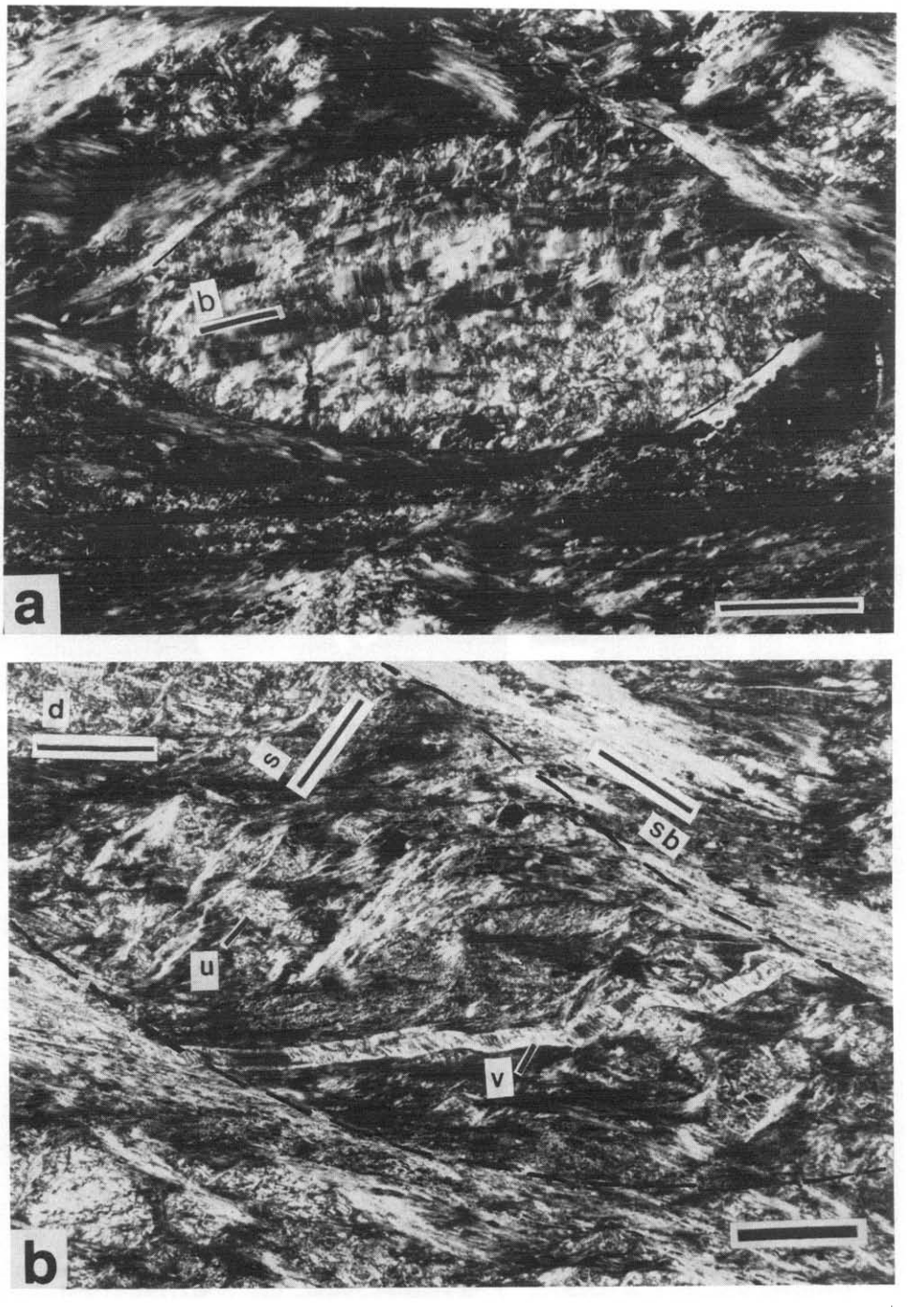

Fig. 4. Examples of lenticular pods. (a) Photomicrograph of lenticular pod composed of bladed mat textured serpentinite and surrounded by mylonitic serpentinite. Incipient brittle faults (b) traverse the pod. Scale bar = 0.4 mm. (b) Photomicrograph of sheared serpentinite showing timing and angular relations of sequential faults and fractures. Degraded lenticular pod (dashed lines) surrounded and cross-cut by dextral shears (d, line shows orientation) and cross-cut by sinistral faults (s). Note that sinistral faults do not extend beyond the lenticular domain or surrounding dextral shears and yet offset and fold the internal dextral shears. The areas between the crossing shears are relatively undeformed (u) and constitute smaller lenticular pods. A cross-fiber serpentine vein (v) was offset along dextral shear bands (sb). Scale bar = 1 mm.

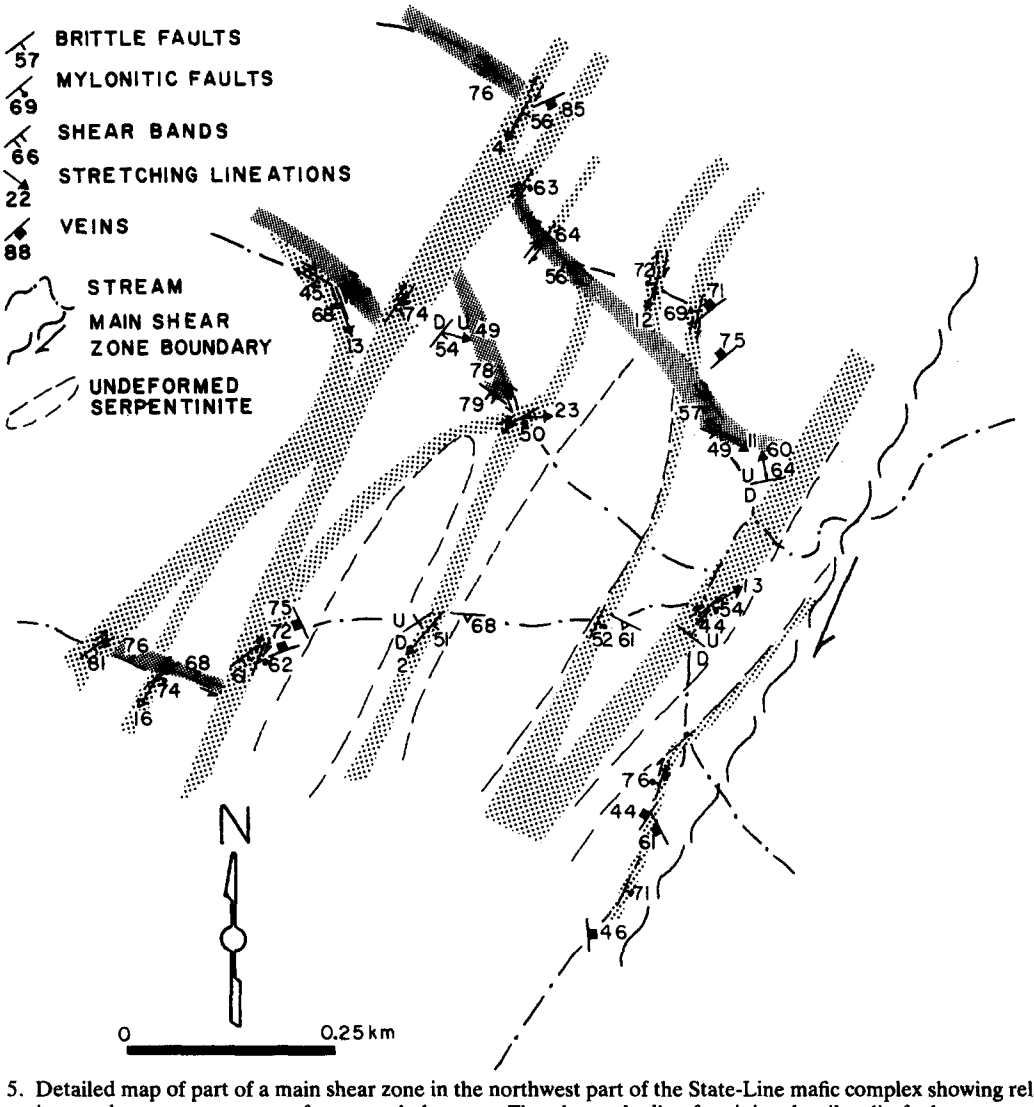

Fig. 5. Detailed map of part of a main shear zone in the northwest part of the State-Line mafic complex showing relative orientations and movement senses of structural elements. Fine dense shading for sinistral strike-slip faults, coarse open shading for dextral strike-slip faults. See Fig. 2 for location of area.

However, the anastomosing nature of both the dextral and sinistral faults and posible rigid rotation of the pods produces a cumulative variation in the orientations of these fold axes. The deformed reverse faults appear to have undergone similar reorientation and are commonly steeply dipping and either moderately NE- or NW-striking and parallel to the dextral and sinistral strike-slip faults, respectively (Fig. 7c).

MOVEMENT HISTORY OF THE SHEAR ZONES

The progression of deformation in the shear zones in the serpentinite of the State-Line complex involved the establishment of anastomosing throughgoing faults and subsequent deformation of the areas between them (Figs. 5 and 8). Spaced dextral transcurrent faults formed an anastomosing pattern in the early stages of shear zone development. The areas between the faults consisted of large lenticular pods of massive, relatively undeformed serpentinite (Fig. 8a). With continued deformation, the established faults widened or in some cases became inactive and new faults formed in the intervening lenticular pods (Fig. 8b). This process served to subdivide the areas between the faults into smaller lenticular pods. At some critical combination of size and stress, the lenticular pods degenerated in a complex sequence of faulting.

The degeneration and fragmentation of the lenticular pods appears to have begun with the formation of N-striking slickensided reverse faults and extensional veins with E–W strikes (Fig. 8a). They were deformed and rotated by both dextral and sinistral strike-slip faults. The veins and reverse faults probably formed concurrently with the bounding dextral strike-slip faults. Dominantly NE-striking splay faults of the widening bounding faults subdivided the lenticular pods into smaller lenticular pods (Fig. 8b). The splay faults may have been generated through Riedel shearing. Some of the splay faults developed into major throughgoing faults whereas others became inactive. Some of the dextral mylonitic faults developed E–W-striking dextral shear bands. Northwest-striking sinistral strike-slip faults transected the lenticular pods and inactive dextral faults, linking

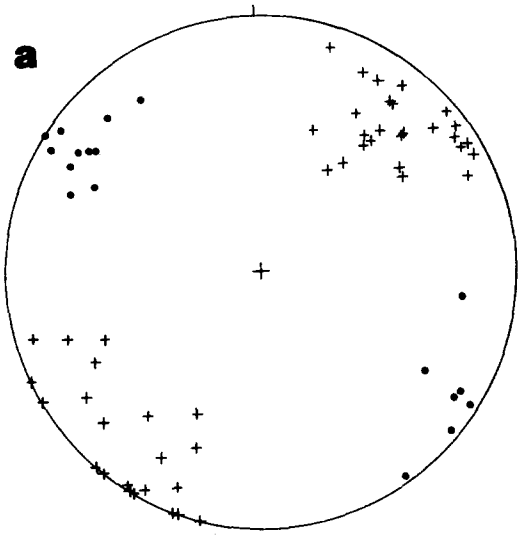

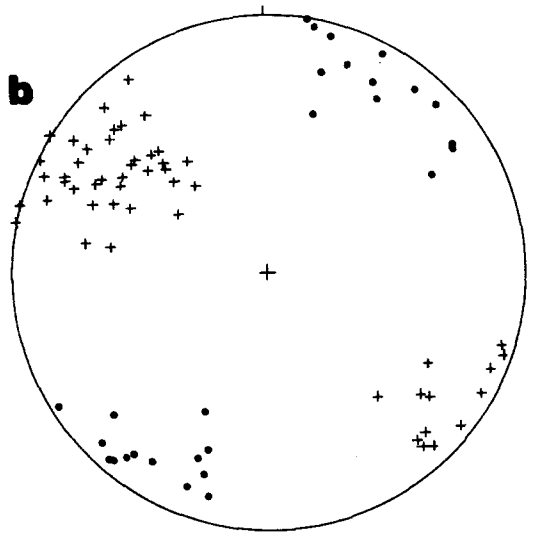

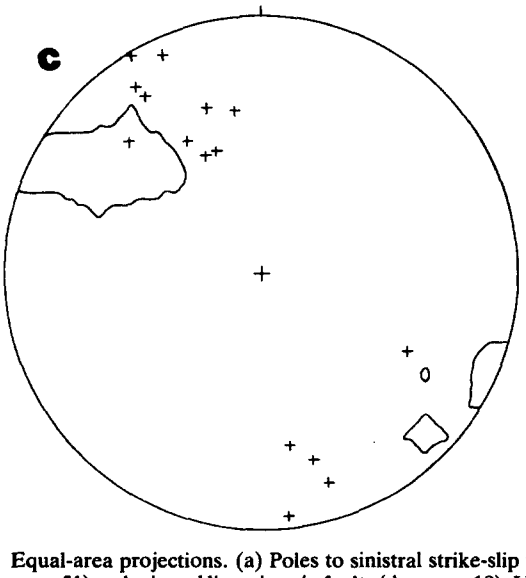

Fig. 6. Equal-area projections. (a) Poles to sinistral strike-slip faults (crosses, $n = 51$) and mineral lineations in faults (dots, $n = 18$). Values are averaged for each outcrop. (b) Poles to least reoriented dextral faults (crosses, $n = 56$) and mineral lineations in faults (dots, $n = 28$). (c) Poles to dextral shear bands (crosses, $n = 14$). The 10% contour per 1% area for least reoriented dextral faults is shown (see b). All values are averaged for each outcrop.

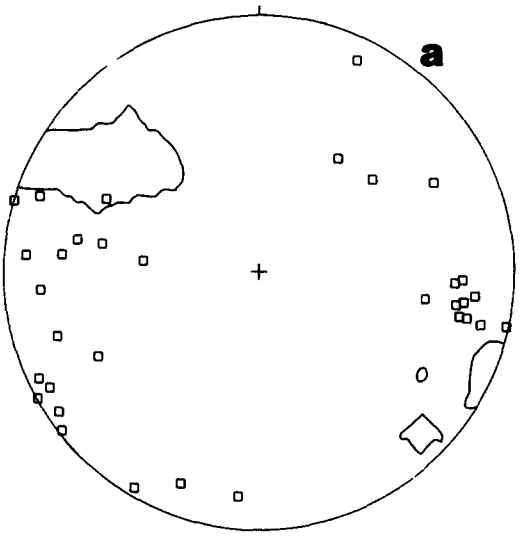

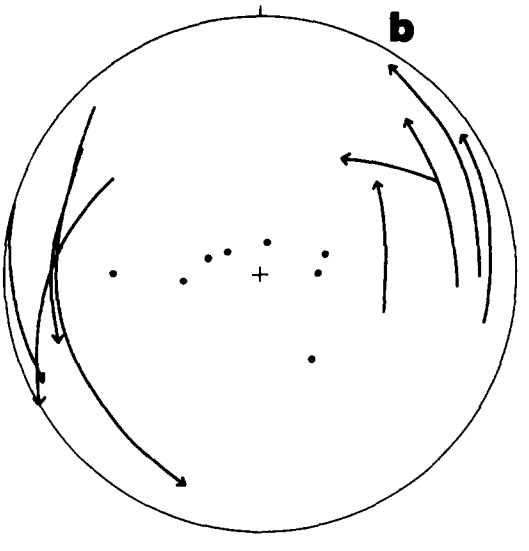

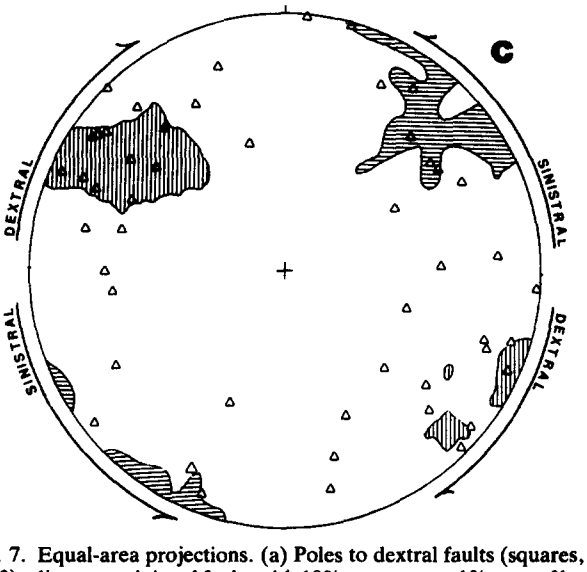

Fig. 7. Equal-area projections. (a) Poles to dextral faults (squares, $n = 33$) adjacent to sinistral faults with 10% contour per 1% area of least reoriented dextral faults. (b) Poles to dextral faults in drag folds adjacent to sinistral faults. Poles are joined along great circles (heavy lines) with arrows pointing towards the sinistral faults. Fold axes of the drag folds (dots) are plotted. (c) Poles to reverse faults (triangles, $n = 49$) with 10% contours per 1% area for dextral faults (vertical lines) and sinistral faults (horizontal lines). Shear drag directions for the strike-slip faults around outside of net (arrows) as labelled.

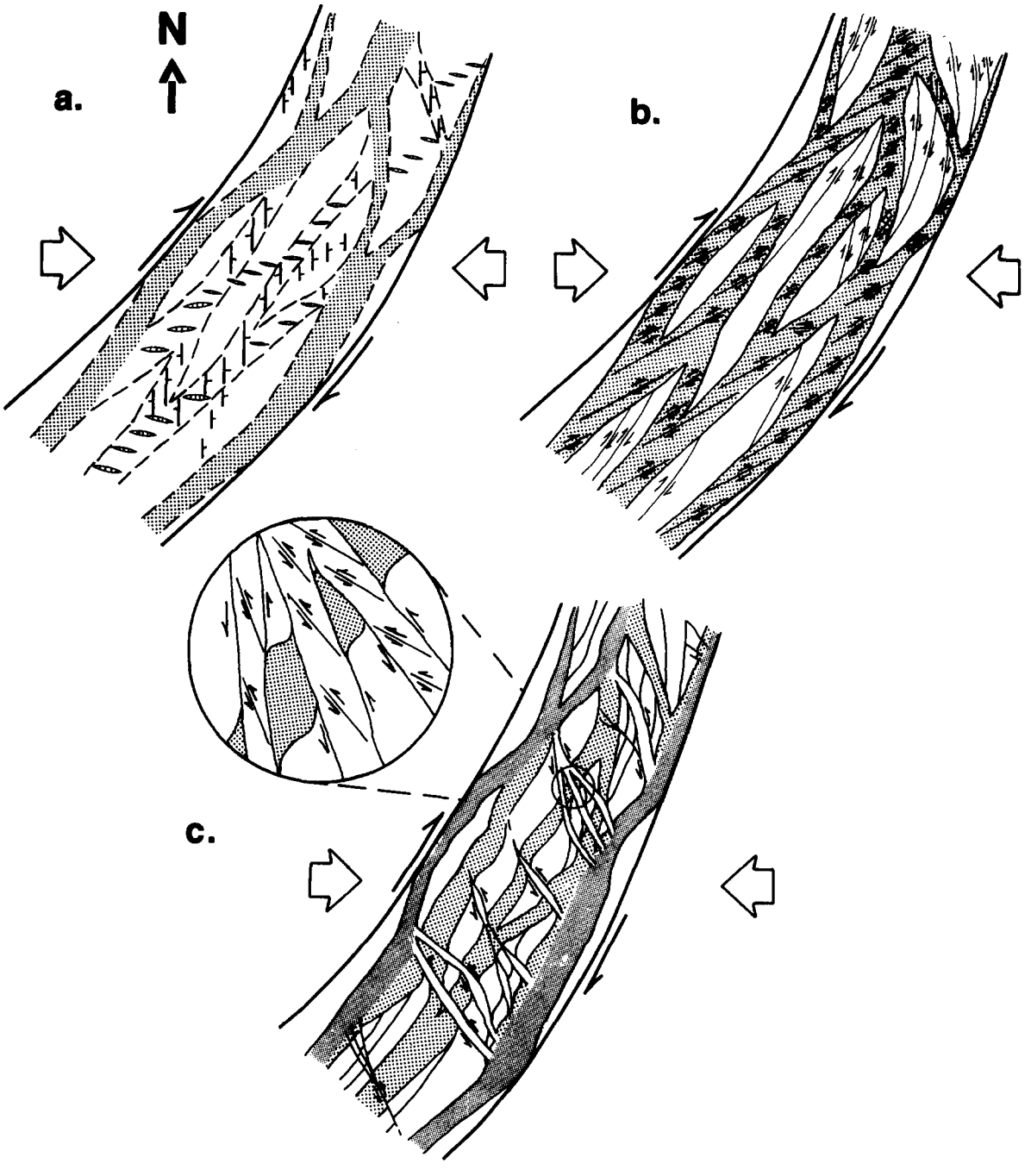

Fig. 8. Model for the sequence of faulting in the main shear zones of the State-Line serpentinite. (a) Incipient dextral shearing along anastomosing faults (shaded bands) and the development of veins (cigar shapes) and reverse faults (lines with dip directions) in lenticular pods (domains). Large arrows indicate maximum compression direction. (b) Dextral strike-slip faulting. Dextral mylonitic faults (shaded bands) and brittle slickensided faults (thin lines with arrows) anastomose within the lenticular domains and continued activity of anastomosing faults. Late dextral strike-slip shear band (lines with arrows within shaded bands) formation within some of the dextral mylonites. (c) Major sinistral strike-slip movement and minor late sinistral shear band development. Mylonitic faults (bands with arrows) and brittle slickensided faults (thin lines) anastomose within the main shear zone. Inactive dextral faults (coarse shaded bands from b) show drag folds. Continued activity of dextral throughgoing faults (fine shaded bands).

the active bounding faults (Fig. 8c). Drag folds formed in the inactive dextral strike-slip faults where they were crossed by the sinistral faults. Sinistral shear bands locally formed in the sinistral strike-slip faults. Based on the retrograde metamorphic reactions in the serpentinite mylonites, activity in the bounding dextral strike-slip faults outlasted all other faults. If shearing had continued, the active mylonitic fault zones would have widened and engulfed the fragmented lenticular pods. The shear zones would consequently appear as continuous bands of mylonite.

The processes responsible for the mesoscopic to megascopic development of the shear zones were also active on the microscopic scale. The flow foliation (cords) anastomoses around elongate lenticular pods (cores) of less deformed bladed mat or mesh textured serpentinite in the mylonitic serpentinite (Figs. 3a and 4a). In many cases, the pods show recrystallization and

drag at their edges. These features are interpreted to reflect reduction of the pods as they were slowly consumed in the expanding mylonitic foliation. In other cases, the pods were fragmented in a similar sequence of faulting to that observed on the map scale (Fig. 4b), in a manner similar to the brittle failure of a feldspar grain in a granitic mylonite (see Simpson & Schmid 1983). The fragments were later broken down and assimilated into the mylonitic foliation.

Unlike the bounding faults, the lenticular pods were composed of antigorite-rich serpentinite with nearly isotropic textural distribution. As deformation proceded, each sequential fault type within the pods likely began as a brittle fault and developed into mylonite. This transition involved a metamorphic reaction to lizardite within the mylonite. The crossing faults further partitioned the pods which promoted fragmentation, reaction and ultimate assimilation into the mylonite zone.

The degeneration of the foliation-scale lenticular pods was clearly not synchronous with the degeneration of the map scale pods. The pod in Fig. 4(b) underwent the same sequence of events as the map scale pods, cross-fiber vein formation, dextral faulting and finally sinistral faulting. However, the sinistral faults transected the pod and linked dextral shear bands. On the mesoscopic scale, dextral shear bands are reoriented in drag folds adjacent to sinistral faults. The microscopic and mesoscopic sinistral faults could not have formed synchronously. Therefore, the relative timing of faulting within a lenticular pod is specific to that pod. Each pod apparently acted as an independent system within the constraints of the shear zone system.

A possible additional process in the development of the shear zones is rigid body rotation. The cross-fiber vein in Fig. 4(a) has clearly undergone relative rotation from its original orientation. Most of this rotation can be accounted for by internal strain but because the lenticular pod is bounded by faults, rigid body rotation cannot be precluded as a contributing factor. No evidence has been found for rigid rotation on the map scale. Considering, however, that each of the lenticular pods acted as an independent system, interacted with other pods and was bounded by faults, some rotation would be expected and may contribute to the variability in fault orientations.

CONCLUSIONS

The serpentinite portion of the State-Line complex is deformed by a series of 0.2–1.4 km wide dextral strike-slip shear zones. These zones are composed of anastomosing throughgoing mylonitic faults and the variably deformed lenticular-shaped areas between the faults. The throughgoing faults are relatively wide and exhibit a long, relatively simple history. The lenticular areas, on the other hand, display a complex sequence of faulting. The sequence began with brittle reverse faulting and joint formation followed by ductile dextral strike-slip faulting and conjugate sinistral strike-slip faulting. A similar sequence occurred in microscopic lenticular pods within mylonite, but was clearly not synchronous with that in the mesoscopic and megascopic lenticular pods. Each lenticular pod may have acted as a separate system.

Acknowledgements—Funding was provided through a grant from the Pennsylvania Department of Environmental Resources and a Henry Rutgers Research Fellowship. Thanks to F. J. Wicks and D. S. O'Hanley for reviews of an early version of the manuscript. The reviews of A. Bobyarchick, C. Simpson, S. Treagus and an anonymous reviewer greatly improved the later manuscript, and are appreciated.

REFERENCES

Berthé, D., Choukroune, P. & Jegouzo, P. 1979. Orthogneiss mylonite and non-coaxial deformation in granites: the example of the south Armorican shear zone. *J. Struct. Geol.* **1**, 31–42.

Crowley, W. P. 1976. The geology of the crystalline rocks near Baltimore and its bearing on the evolution of the eastern Maryland Piedmont. *Maryland Geol. Surv. Rept. of Inv.* **27**, 1–40.

Gates, A. E. In press. Shear zone control on mineral deposits in the State-Line serpentinite. In: *Applications to Exploration* (edited by Petruk, W., Vassiliou, A. H. & Hausen, D.). *Ore Geol. Rev.* **3**.

Gates, A. E. & Kambin, R. C. 1990. Comparison of the natural deformation of the State-Line serpentinite, U.S.A., with experimental studies. *Tectonophysics* **182**, 249–258.

Gates, A. E., Muller, P. D. & Valentino, D. W. In press. Terranes and tectonics of the Maryland and southeast Pennsylvania Piedmont. In: *Field Trip Guide for the 1991 Northeast/Southeast Geological Society of American Meeting* (edited by Schultz, A. P.). Virginia Museum Publ.

Gates, A. E., Simpson, C. & Glover, L., III. 1986. Appalachian Carboniferous dextral strike-slip faults: an example from Brookneal, Virginia. *Tectonics* **5**, 119–133.

Gates, A. E. & Sun, D. F. 1989. Geological and geophysical evidence for thrust faulting in the Taconic suture zone of the southeastern PA Piedmont. *Geol. Soc. Am. Abs. w. Prog.* **21**, 17.

Hanan, B. B. & Sinha, A. K. 1989. Petrology and tectonic affinity of the Baltimore mafic complex, Maryland. In: *Ultramafic Rocks of the Appalachian Piedmont* (edited by Mittwede, S. K. & Stoddard, E. F.). *Spec. Pap. geol. Soc. Am.* **231**, 1–18.

Katz, M. B. 1986. Tectonic analysis of faulting at Woodsreef asbestos mine and its possible relationship to the kinematics of the Peel fault. *Aust. J. Earth Sci.* **33**, 99–105.

Lapham, D. M. & Bassett, W. A. 1964. K–Ar dating of rocks and tectonic events in the Piedmont of southeastern Pennsylvania. *Bull. geol. Soc. Am.* **75**, 661–668.

Maltman, A. J. 1978. Serpentinite textures in Anglesey, North Wales, United Kingdom. *Bull. geol. Soc. Am.*, **89**, 972–980.

Morgan, B. A. 1977. The Baltimore Complex, Maryland, Pennsylvania and Virginia. In: *North American Ophiolites* (edited by Coleman, R. G.). *Bull. Oregon Dept Geol. Miner. Ind.* **95**, 41–49.

Norrell, G. T., Teixell, A. & Harper, G. D. 1989. Microstructure of serpentinite mylonites from the Josephine ophiolite and serpentinization in retrogressive shear zones, California. *Bull. geol. Soc. Am.* **101**, 673–682.

O'Hanley, D. S. 1987. The origin of the chrysotile asbestos veins in southeastern Quebec. *Can. J. Earth Sci.* **24**, 1–9.

O'Hanley, D. S. 1988. The origin of alpine peridotite-hosted, cross fiber, chrysotile asbestos deposits. *Econ. Geol.* **83**, 256–265.

Shaw, H. F. & Wasserburg, G. J. 1984. Isotopic constraints on the origin of Appalachian mafic complexes. *Am. J. Sci.* **284**, 319–349.

Simpson, C. & Schmid, S. M. 1983. An evaluation of criteria to deduce the sense of movement in sheared rocks. *Bull. geol. Soc. Am.* **94**, 1281–1288.

Wagner, M. E. & Srogi, L. 1987. Early Paleozoic metamorphism at two crustal levels and a tectonic model for the Pennsylvania–Delaware Piedmont. *Bull. geol. Soc. Am.* **99**, 113–126.

Wicks, F. J. & Whittaker, E. J. W. 1977. Serpentine textures and serpentinizations. *Can. Miner.* **15**, 459–488.

Williams, A. J. 1979. Foliation development in serpentinites, Glenrock, New South Wales. *Tectonophysics* **58**, 81–95.